

Short note

Strong reaction channels at barrier energies in the system ${}^6\text{Li} + {}^{208}\text{Pb}$

C. Signorini^{1,a}, M. Mazzocco¹, G.F. Prete², F. Soramel³, L. Stroe¹, A. Andrighetto¹, I.J. Thompson⁴, A. Vitturi¹, A. Brondi⁵, M. Cinausero², D. Fabris¹, E. Fioretto², N. Gelli⁶, J.Y. Guo^{1,7}, G. La Rana⁵, Z.H. Liu⁷, F. Lucarelli⁶, R. Moro⁵, G. Nebbia¹, M. Trotta², E. Vardaci⁵, and G. Viesti¹

¹ Physics Department and INFN, via Marzolo 8, I-35131 Padova, Italy

² INFN, Laboratori Nazionali di Legnaro, I-35020 Legnaro, Italy

³ Physics Department and INFN, I-33100 Udine, Italy

⁴ Physics Department, University of Surrey, Guilford GU2 5XH, U.K.

⁵ Physics Department and INFN, I-80125 Napoli, Italy

⁶ Physics Department and INFN, Firenze, Italy

⁷ China Institute of Atomic Energy, Beijing, P.R. of China

Received: 15 January 2001 / Revised version: 16 February 2001

Communicated by J. Äystö

Abstract. Large cross-section reaction channels were measured in the systems ${}^6\text{Li}({}^7\text{Li}) + {}^{208}\text{Pb}$ with high statistical accuracy at 5(3) energies around the Coulomb barrier from 29 to 39 MeV. These channels were assigned (mainly) to the breakup of ${}^6\text{Li}$, very loosely bound, into $\alpha + d$ and to the breakup of ${}^5\text{Li}$, produced by n-transfer to the target, into $\alpha + p$ and to similar processes with ${}^7\text{Li}$ beam. The cross-sections with ${}^6\text{Li}$, $S_\alpha = 1.475$ MeV, are systematically larger than the ${}^7\text{Li}$ ones. This reflects, most likely, the higher binding energy of ${}^7\text{Li}$, $S_\alpha = 2.468$ MeV. Theoretical predictions for the ${}^6\text{Li} + {}^{208}\text{Pb}$ system which include for ${}^6\text{Li}$ breakup to continuum states within a continuum discretized coupled-channels approach (CDCC) and resonant breakup plus n-transfer with DWBA reproduce the angular distribution shapes but still underestimate the cross-sections by a factor ~ 3 .

PACS. 25.70.Ji Fusion and fusion-fission reactions – 25.70.Mn Projectile and target fragmentation – 24.10.Eq Coupled-channel and distorted wave models

The study of breakup (BU) processes at energies around the Coulomb barrier has recently attracted much interest when it involves nuclei that have halo or skin structures, or that are weakly bound, especially in connection with ongoing and planned research with radioactive ion beams. In fact it is expected, on the basis of very straightforward arguments, that the BU processes for such weakly bound nuclei have a large cross-section. This should strongly influence fusion around the barrier. Many theoretical works have been presented on this topic, with conflicting predictions since both enhanced and hindered cross-sections have been calculated.

Very strong reaction channels were observed at the barrier in the systems ${}^6\text{He} + {}^{209}\text{Bi}$ [1] and ${}^9\text{Be} + {}^{208}\text{Bi}$ [2]. They were assigned to α -particles originating from projectile BU + neutron(s) transfer. The connection of this strong process with the fusion of halo/skin nuclei [3,4]

around the barrier is under study. Moreover the elastic scattering of ${}^9\text{Be}$ by ${}^{209}\text{Bi}$ [5] has an anomalous potential most likely due also to this strong reaction channel. Large reaction cross-sections are reported also from the analysis of the elastic scattering of ${}^6\text{He}$ by ${}^{209}\text{Bi}$ [6] and ${}^{12}\text{C}$ [7]. On the contrary the ${}^{17}\text{F} + {}^{208}\text{Pb}$ system seems to have a small BU cross-section [8] at 170 MeV, twice the Coulomb barrier, and theoretical calculations foresee [9] even a smaller BU cross-section at the barrier.

We decided to study BU effects in the system ${}^6\text{Li} + {}^{208}\text{Pb}$ for the following reasons: 1) ${}^6\text{Li}$ is the most weakly bound stable nucleus with $S_\alpha = 1.475$ MeV, 2) ${}^6\text{Li}$ beam can be produced with good intensity, allowing data to be obtained with high statistical accuracy, 3) any process where ${}^6\text{Li}$ breaks produces one α -particle (plus eventually d or p) easy to be detected, 4) the elastic scattering of this system was measured with high accuracy at several energies around the barrier [10] so that the optical model parameters are well known. Data were collected also for

^a e-mail: signorini@pd.infn.it

the system ${}^7\text{Li} + {}^{208}\text{Pb}$ ($S_\alpha = 2.468$ MeV). In this case the ~ 1 MeV higher binding energy should have the effect of producing a BU cross-section lower than for ${}^6\text{Li}$, as already predicted [11].

The main goal of this experiment was to search for the strong reaction channels expected, most likely originating from the α -particles produced by the ${}^6\text{Li}$ BU, and to measure the inclusive cross-section for such α -particles production.

The experiment was done at the Tandem Van de Graaff accelerator of the Laboratori Nazionali di Legnaro with Li beams of 1 pnA and a Pb enriched target of $150 \mu\text{g}/\text{cm}^2$ thickness backed by a carbon foil of $10 \mu\text{g}/\text{cm}^2$. The data were collected with ${}^6\text{Li}$ (${}^7\text{Li}$) at 29, 31, 33, 35, 39 MeV (29, 33, 39 MeV). The emitted charged particles were detected with a 4π array of Si + CsI(Tl) telescopes, described in detail in ref. [12]. The array is essentially made of two parts: a “wall” in forward directions, covering the angles from 2.5° to 34° and a “ball” part covering the remaining angles up to 163° . In the present experiment only the “ball” part was needed since from the ${}^6\text{Li} + {}^{208}\text{Pb}$ kinematics the grazing angles are $> 60^\circ$. The “ball” consists of 18 segments covering all the 2π azimuthal angle, each segment is made of 7 detectors covering the angles from 34° to 163° . Each single detector is located at 15 cm from the target, spans an angle of $\sim 20^\circ(\theta) \times 17^\circ(\phi)$ corresponding to solid angles ranging from 32 msr in the backward angles to 79 msr at $\sim 90^\circ$ and consists of a ΔE silicon detector, $300 \mu\text{m}$ thick, backed by a CsI scintillator 5 mm thick. The ΔE detector can stop up to 25 MeV α -particles. This system allows a very good identification of light charged particles: α , triton, deuteron and proton. The data-taking was arranged in order to record for each telescope the ΔE spectra and the ΔE vs. E_{res} matrices for particle identification within the ΔE detector capabilities. Coincidences between the various telescopes were not considered in this first experiment because not necessary for its goal, *i.e.* measurement of the inclusive α -particle production cross-section; this is essentially equal to the total BU cross-section since every BU event produces one α -particle. Moreover the large opening of the detectors does not warrant enough angular resolution because the α -d (-p) cone is around $20^\circ(25^\circ)$.

The absolute cross-sections were obtained by normalizing each single spectrum with its own elastic peak; these absolute cross-sections are reported in ref. [10]. An additional check was done with the pure Rutherford cross-section measured in two monitors located at $\pm 30^\circ$ to the beam direction, with an opening angle of 0.9° , covering a solid angle of 0.19 msr. Figure 1a shows a typical ΔE spectrum observed in a detector located from 68° to 85° to the beam at 35 MeV. Figure 1b displays the corresponding $\Delta E - E_{\text{res}}$ two-dimensional spectrum which shows the production of α , deuteron and proton. The broad peak in fig.1a, with energies ranging from 16 to 25 MeV, has an average energy of ~ 21 MeV, which corresponds to 2/3 of the elastic peak one, and has a large width typical of three-body kinematics; it was therefore attributed to α -particles emitted in the reaction also for the arguments presented

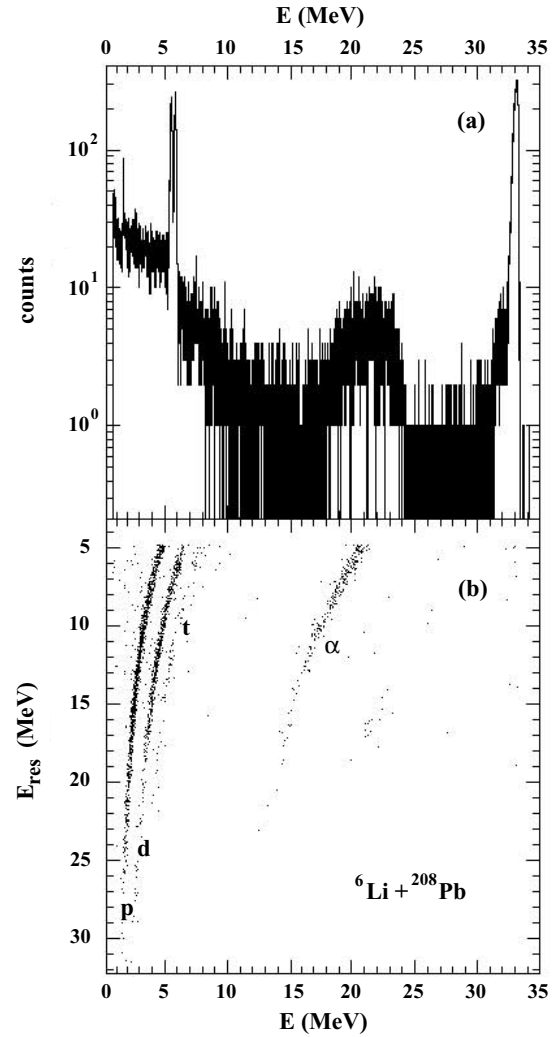


Fig. 1. System ${}^6\text{Li} + {}^{208}\text{Pb}$ at $E_{\text{beam}} = 35$ MeV, detector angle from 68° to 85° : a) Spectra of charged particles observed in the ΔE Silicon detector. The broad peak at around 21 MeV is assigned to the α -particles emitted by the reaction; it is broad because of the three-body kinematics. The peak at 33 MeV is from ${}^6\text{Li}$ elastic scattering. The strong peaks at ~ 5.5 MeV are from an α calibration source. b) Two-dimensional spectrum ΔE vs. E_{res} ; α , deuteron and protons are clearly evidenced. The energy calibration of the E_{res} scale apply only to α -particles due to the non equal response of the CsI detector to particles with different atomic numbers. The cut-off at E_{res} less than ~ 4.5 MeV was made because of the electronic noise in the CsI detectors.

in the following. Two processes are most likely to produce this channel: the first is the direct BU of ${}^6\text{Li} + {}^{208}\text{Pb}$ into $\alpha + d$, while the second is the BU of the unbound ${}^5\text{Li}/(p + \alpha)$ produced by the n-transfer reactions ${}^{208}\text{Pb}({}^6\text{Li}, {}^5\text{Li}/(p + \alpha)){}^{209}\text{Pb}$ which have Q -values of -1.728 MeV for the ${}^5\text{Li}$ production and of $+0.238$ MeV for $(p + \alpha)$. Under the simplified assumption of pure Coulomb trajectories and of a BU kinematics not influenced by the target nuclear field (*i.e.* with no post acceleration effects) the ${}^6\text{Li}$ BU (n-transfer + BU) produces α -particles ranging from

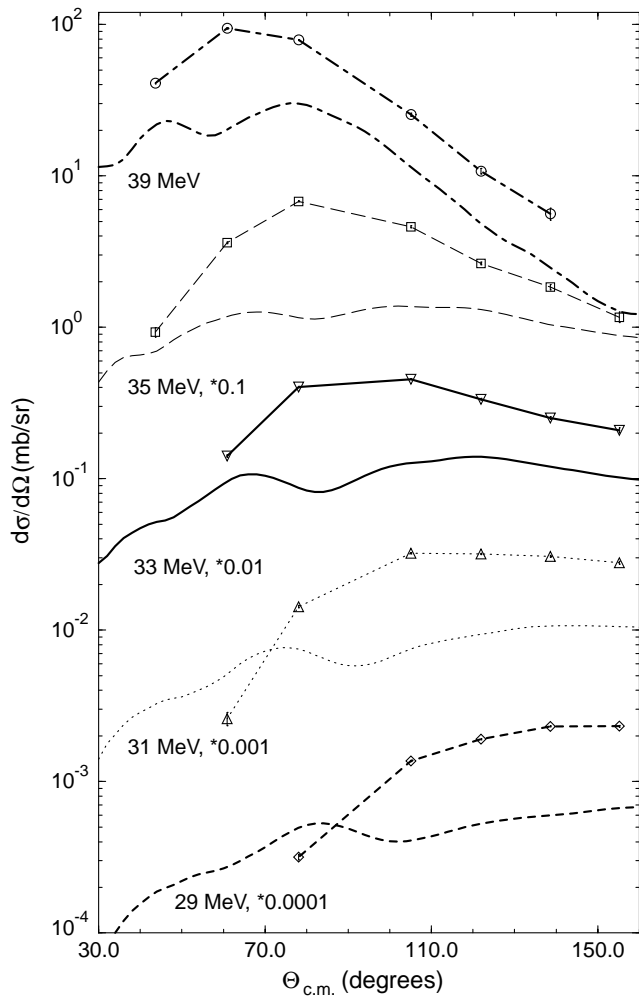


Fig. 2. Experimental and theoretical angular distributions at various energies for the system ${}^6\text{Li} + {}^{208}\text{Pb}$. The experimental points plotted are the average values over the solid angle of the large-area detectors; these points are connected with straight lines to guide the eye.

16(21) MeV to 26(30) MeV and a $d - \alpha$ ($p - \alpha$) cone of $\sim 20^\circ$ (25°). This is in agreement with the experimental observations of fig. 1. In fig. 1b we clearly observe α -particles with energy > 25 MeV punching through the ΔE detector and the protons and deuterons produced by the two BU processes above. A similar broad peak was observed systematically also in the system ${}^9\text{Be} + {}^{209}\text{Bi}$ [2] and was assigned to α -particles from the decay of ${}^8\text{Be}$ produced by ${}^9\text{Be}$ BU and n-transfer.

The measured angular distribution are shown in fig. 2; the differential cross-sections plotted are the average value over the large angular range subtended by each detector. The errors are smaller than 1%. The total inclusive cross-sections for α -particles were evaluated as the sum over all the detectors plus the contribution of the angles not covered by the ball around 90° , in backward and in forward angles; these contributions were extrapolated by a quadratic fit of the measured cross-sections. The ${}^7\text{Li}$ data were evaluated in the same way. The cross-sections ob-

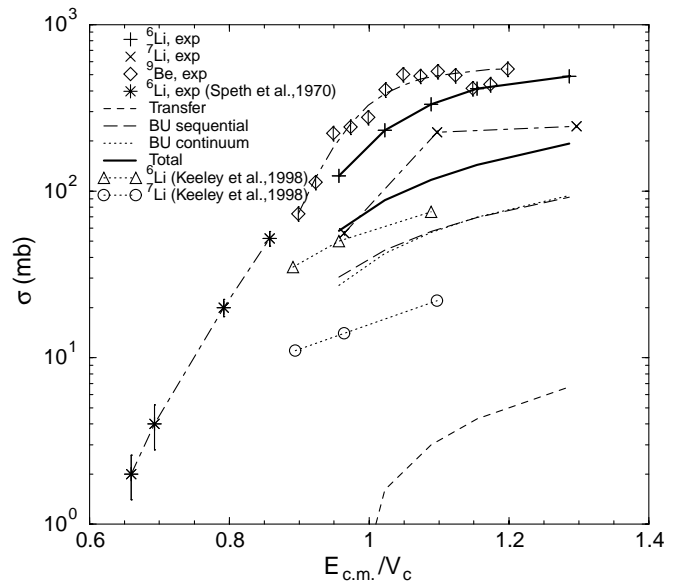


Fig. 3. Total inclusive cross-sections for α -particles: experimental for the systems ${}^{6,7}\text{Li} + {}^{208}\text{Pb}$ and ${}^9\text{Be} + {}^{209}\text{Bi}$, calculated for the system ${}^{6,7}\text{Li} + {}^{208}\text{Pb}$. The data are plotted versus $E_{c.m.}/V_c$, with V_c Coulomb barrier, for a better comparison among the different nuclei. V_c used for ${}^9\text{Be}$ is 38.4 MeV [13] and for ${}^{6,7}\text{Li}$ 29.5 and 29.1 MeV, respectively. The experimental points are connected with lines to guide the eye.

tained are shown in fig. 3; the errors are smaller than 5%. The largest uncertainty originates from the extrapolation of the angular distributions to low cross-sections in forward directions. Contributions from α -particle evaporation after the fusion of ${}^6\text{Li}$ with the carbon backing nuclei are to be excluded since expected at much lower energies and checked at some energies with a carbon target. There might be a possible contribution from α -particles evaporating from the (${}^6\text{Li} + {}^{208}\text{Pb}$) compound nucleus expected [14] around 21 MeV. This cross-section was estimated to be at least one order of magnitude smaller than the BU one from: i) the cross-sections for the production of evaporation residues measured during a calibration run (unpublished data) by our group at the INS (Tokyo) Cyclotron in the ${}^7\text{Li} + {}^{209}\text{Bi}$ system in the energy range 29 to 48 MeV, ii) the evaporation calculations with both PACE2 and CASCADE codes. Moreover the angular distributions shown in fig. 2 are peaked around the grazing angle; this supports a surface interaction mechanism, *i.e.* BU, rather than evaporation. Figure 3 shows also: i) similar data for the system ${}^6\text{Li} + {}^{208}\text{Pb}$ at lower energies [15] matching well our results, ii) data for the similar system ${}^9\text{Be} + {}^{209}\text{Bi}$ [2].

The ${}^6\text{Li}$ BU cross-sections as well as the ${}^9\text{Be}$ ones are quite large; this confirms our expectation which motivated this work. The ${}^7\text{Li}$ projectile has cross-sections systematically lower than ${}^6\text{Li}$, most likely because of its binding energy ~ 1 MeV higher than ${}^6\text{Li}$; this is in agreement with the calculations of ref. [11] also reported in fig. 3. ${}^9\text{Be}$ projectile has rather an opposite, and somehow unexpected, behavior since, even if its binding energy is ~ 0.2

MeV higher than ${}^6\text{Li}$, the cross-sections are well above the ${}^6\text{Li}$ ones. A tentative explanation could be that the structure of these two nuclei is quite different: ${}^9\text{Be}$, due to its ${}^8\text{Be}$, 2 α , core is much more deformed (and breakable?). This, anyhow, needs further investigation in any case.

We have made exploratory calculations in order to explain the ${}^6\text{Li}$ results in the framework of a dynamical reaction theory based on coupled-channels methods, with inclusion of coupled discretized continuum channels (CDCC) and DWBA formalisms in order to take into account this new feature of weakly bound nuclei, namely the BU. Our purpose was to show that there is something interesting also from a theoretical viewpoint about the data. We have considered BU to continuum unbound states in ${}^6\text{Li}$ as well as to resonant unbound ones (the so-called sequential BU). As mentioned above the α emission is believed to have two origins: direct ${}^6\text{Li}$ BU and ${}^5\text{Li}$ BU following n-transfer. We have therefore adopted a mixed approach within the code FRESKO [16]. The continuum BU was calculated in the CDCC formalism by using an α -d cluster structure for the ground and continuum states. As a first tentative approach the α -d continuum region in ${}^6\text{Li}$ above the α threshold was subdivided in 10 bins equally spaced, with respect to the momentum of the α -d relative motion, from 1.5 MeV up 6.5 MeV, and the unit spin of deuteron was neglected. Only monopole and quadrupole couplings were included, with both direct continuum coupling and continuum-to-continuum coupling. The following Woods-Saxon potential parameters were adopted for the real part of the α - ${}^{208}\text{Pb}$ (d- ${}^{208}\text{Pb}$) interaction: $V_0 = 20.0$ (78.3) MeV, $r_0 = 1.220$ (1.336) fm, $a_0 = 0.57$ (0.79) fm. For the imaginary part of the α - ${}^{208}\text{Pb}$ system we adopted a volume term with $W_i = 38.0$ MeV, $r_i = 1.22$ fm, $a_i = 0.5$ 7fm and for the d- ${}^{208}\text{Pb}$ system a surface term with $W_s = 16.6$ MeV, $r_s = 1.47$ fm, $a_s = 0.598$ fm. All these values were extracted from the tabulation of ref. [17]. The calculations reproduce fairly well the elastic scattering angular distributions at the various energies [10].

The transfer + sequential BU was calculated in a simplified DWBA approach. For the sequential BU part we included only the following two excited levels in ${}^6\text{Li}$ [18]: 2.186 MeV, 3^+ , $\delta_2 = 4.13$ fm, $\beta_2 = 1.6$, and 4.310 MeV, 2^+ , $\delta_2 = 2.24$ fm, $\beta_2 = 0.9$ (δ_2 is the deformation length of the potential). Both levels are unbound and should be the main responsible of the sequential BU. In principle levels with these two energies are already counted for in the CDCC approach, but were non-resonant, and they have cross-sections ranging from 2 mb, at 29 MeV, to 11 mb, at 39 MeV; this is small compared to the values calculated within the DWBA approach ranging from 27 mb to 86 mb. Since only the DWBA approach as yet includes the 3^+ and 2^+ resonances, as a first approximation we simply add the resonant and non-resonant contributions from the CDCC and DWBA models, respectively. For the transfer we have included the first 7 levels in ${}^{209}\text{Pb}$. They are well known to be of single-particle nature and are all well excited in the (${}^9\text{Be}$, ${}^8\text{Be}$) n-transfer reaction [19] at 50 MeV: $9/2^+$, 0.0 MeV; $11/2^+$, 0.78 MeV; $15/2^-$, 1.42 MeV; $5/2^+$, 1.57 MeV; $1/2^+$, 2.03 MeV; $7/2^+$, 2.49 MeV;

Table 1. Woods-Saxon potential parameters adopted for the DWBA calculations at the various energies for the system ${}^6\text{Li} + {}^{208}\text{Pb}$.

E_{beam} (MeV)	V_0 (MeV)	r_0 (fm)	a_0 (fm)	W_i (MeV)	r_i (fm)	a_i (fm)
29	30.21	1.191	0.684	30.82	1.30	0.654
31	33.99	1.191	0.684	22.73	1.30	0.675
33	28.86	1.191	0.684	12.44	1.30	0.778
35	24.34	1.191	0.684	12.76	1.30	0.783
39	23.50	1.191	0.684	11.63	1.30	0.819

$3/2^+$, 2.54 MeV. For all these levels we have assumed a transfer amplitude equal to 1 since they are of rather pure single-particle nature. At each energy we have adopted a potential of Woods-Saxon shape deduced with the following procedure. The real part was calculated with the folding model via M3Y interaction + tabulated matter densities, as in ref. [10], and then fitted with a W-S shape; the imaginary parameters were taken from ref. [10]. All the parameters adopted, which well reproduce all the experimental elastic scattering cross-sections, are listed in table 1.

The 1p-transfer reaction ${}^{208}\text{Pb}({}^6\text{Li}, {}^5\text{He}/(n + \alpha)){}^{209}\text{Bi}$ was not considered since expected to have a cross-section lower than the 1n-transfer one. This was checked anyhow at 33 MeV: the total 1p-transfer to the first three ${}^{209}\text{Bi}$ levels was calculated to be 0.2 mb, with the same DWBA approach, while the 1n-transfer is 3.0 mb.

The global results, *i.e.* the sum of the three angular distribution originating from continuum BU, sequential BU and 1n-transfer are compared with the experimental α angular distributions in fig. 2; the overall trends are generally reproduced but the absolute values are underestimated by a factor ~ 3 .

In fig. 3 we show the total cross-sections for these three different components as well as their sum. The continuum and sequential BU contribute in the same amount to the total cross-section while the transfer BU has a negligible contribution. Many of the parameters utilized were deduced from experimental data, namely, all the various potentials and the sequential BU transition strengths, so there are not too many degrees of freedom left from this side to the theoretical estimates. The fact that the experimental total cross-sections are still underpredicted means that something is still missing in our theoretical approaches. This is most likely to be dipole breakup, either nuclear dipoles into p -waves of relative α -d motion, or Coulomb + nuclear breakup into s and d -waves continuum states of p - ${}^5\text{He}$ and n - ${}^5\text{Li}$ motion. These last two breakup modes are beyond the present range of CDCC models based on α -d clustering, and will be the subject of future theoretical investigation.

Figure 3 shows also the results of previous calculations [8] done for both ${}^6, {}^7\text{Li}$ projectiles: ${}^6\text{Li}$ results are similar to ours.

In summary the inclusive, large cross-sections for the α -particles production in the systems ${}^6\text{Li}({}^7\text{Li}) + {}^{208}\text{Pb}$

were measured with high statistical accuracy at several energies around the Coulomb barrier. The ${}^6\text{Li}$ system has cross-sections systematically larger than the ${}^7\text{Li}$ one; this was attributed to its binding energy ~ 1 MeV higher than for ${}^6\text{Li}$. The ${}^9\text{Be}$ projectile shows an opposite, unexpected behavior maybe due to structure effects, which needs further investigation. CDCC and DWBA calculations with most parameters deduced from experimental data reproduce the angular distribution shapes but underestimate by a factor ~ 3 the absolute values, and appear to indicate that important dipole modes have yet to be described accurately. We anticipate that investigation of these dipole modes will also cast light on near-barrier breakup of weakly bound nuclei.

The large ${}^6\text{Li}$ BU cross-section should have some influence onto the fusion one. But opposite effects are predicted: enhancement because of coupling to excited states, hindrance because the BU process could simply remove flux from the fusion. The measurement of the ${}^6\text{Li}+{}^{208}\text{Pb}$ fusion cross-section would be therefore very important.

After this manuscript was submitted a publication on the same topic of this work appeared [20]. Also this paper reports large inclusive breakup cross-sections rising smoothly with energy for both ${}^6,{}^7\text{Li}$ projectiles. The cross-sections at 29 MeV are equal to ours within errors, but at 39 MeV the values reported by [20] are a factor ~ 2.6 smaller than ours. The reason of this discrepancy at high energy is not clear and a new experiment is welcome to solve this problem.

References

1. E.F. Aguilera *et al.*, Phys. Rev. Lett. **84**, 5058 (2000).
2. C. Signorini *et al.*, *Proceedings of the International Conference BO2000, Bologna, Italy, May 2000*, edited by D. Vretenar *et al.* (World Scientific, Singapore) in press.
3. M. Trotta *et al.*, Phys. Rev. Lett. **84**, 2342 (2000).
4. J.J. Kolata *et al.*, Phys. Rev. Lett. **81**, 4580 (1998).
5. C. Signorini *et al.*, Phys. Rev. C **61**, 061602(R) (2000).
6. J.J. Kolata, *Proceedings of the International Conference RIB00, Hayama, Japan, November 2000*, edited by T. Nakamura, to be published in Eur. Phys. J. A and Aguilera *et al.*, submitted to Phys. Rev. C.
7. A.N. Ostrowski *et al.*, Phys. Rev. C **60**, 064603 (1999).
8. J.F. Liang *et al.*, Phys. Lett. B **491**, 23 (2000).
9. K.E. Rehm *et al.*, Phys. Rev. Lett. **81**, 3341 (1998).
10. N. Keeley *et al.*, Nucl. Phys. A **571**, 326 (1994).
11. N. Keeley, K. Rusek, Phys. Lett. B **427**, 1 (1998).
12. G. Prete *et al.*, Nucl. Instrum. Meth. Phys. Res. A **422**, 263 (1999).
13. C. Signorini *et al.*, Eur. Phys. J. A **5**, 7 (1999).
14. A.L. Caraley *et al.*, Phys. Rev. C **62**, 054612 (2000).
15. E. Speth *et al.*, Phys. Rev. Lett. **24**, 1493 (1970).
16. I.J. Thompson, Comput. Phys. Rep. **7**, 167 (1988).
17. C.M. Perey, F.G. Perey, Nuclear Data Tables **17**, 1 (1976).
18. F. Ajenberg-Selove, Nucl. Phys. A **480**, 1 (1988).
19. D.P. Stahel *et al.*, Phys. Rev. C **16**, 1436 (1977).
20. G.R. Kelly *et al.*, Phys. Rev. C **63**, 024601 (2000).